Journal of Ovonic Research Vol. 20, No. 6, November - December 2024, p. 803 - 811

Improved structural and dielectric traits of Cd-Zn spinel ferrites by co-substitution of La^{3+} and Er^{3+} cations

Y. M. Alanazi [a], M. I. Arshad [b], N. Amin [b], N. U. Khan [b], N. Sabir [b], M. Naveed [b], A. Saleem [b], S. Mumtaz [c], M. A. U. Nabi [b,*]

[a] *College of Engineering, Chemical Engineering Department, King Saud University Riyadh, Saudi Arabia*

[b] *Department of Physics, Government College University, Faisalabad, 38000, Pakistan*

[c] *Electrical and Biological Physics, Kwangwoon University, Seoul 01897, South Korea*

In the present work, the effect of co-doping of rare earth (Re^{3+}), La and Er cations on the physical and dielectric performance of Cd-Zn spinel ferrites fabricated by sol-gel auto combustion method is reported. The prepared ferrites were doubly calcinated at 550 °C and 750 °C for 2 hours and 8 hours, respectively. The obtained samples were investigated using XRD, FTIR and dielectric measurements. XRD powder patterns verified the single-phase growth of spinel structure of all the as-synthesized ferrites with Fd-3m space group. The obtained results revealed that the Lattice constant reduces with increasing Er^{3+} concentrations, while crystallite size showed increasing behavior with increasing Er^{3+} concentration. FTIR results revealed the existence of two major absorption bands i.e. low frequency bands in range 405-428 cm^{-1} and high frequency bands in range 523- 550 cm^{-1} which are evidence of spinel structure formation. LCR measurements are used to investigate the impact of co-doping of La^{3+} and Er^{3+} on the various dielectric parameters of prepared samples in response to frequency. Dielectric constant and loss decreased with the incorporation of Er^{3+}, while an increase in ac conductivity was observed. The observed properties reveal that the prepared materials are suitable candidates for application in the high-speed microwave and radio frequency devices.

(Received August 31, 2024; Accepted November 14, 2024)

Keywords: La & Er Co-substituted Cd-Zn ferrites, Structural, XRD, FTIR, Dielectric properties

1. Introduction

Ferrite materials are significant category of magnetic materials which are composed of oxygen ions containing ferric ions as their main constituents. They are ceramic magnetic materials and occur in various crystalline structures, however, spinel structure is one of them which has been studied and reported extensively. The idea of spinel structure was taken from $MgAl_2O_4$ [1]. This structure is composed of oxide ions structured in closed-pack FCC form and has two genres of interstitial sites i.e. tetrahedral and octahedral sites. The spinel ferrites contain general formula AB_2O_4, where ‘A’ and ‘B’ represents the divalent and trivalent metal cations on the tetrahedral and octahedral sites respectively [2]. These materials have gained a huge attention of researchers to investigate theirstructure, and the electrical, dielectric and magnetic traits to utilize them in various technological applications. The spinel ferrites are categorized as soft magnetic materials and contain high permeability [3], great chemical stability, large surface area, superior electrical resistivity and low cost [4] and low eddy current loss [5], which can be modified and functionalized easily using various techniques mentioned in the upcoming discussion. Due to above properties, these materials have significant importance for fabrication of recording heads, data storage devices, wave absorbers, electronic devices, high speed microwave and radio frequency devices [6-9].

---

[*] Corresponding author: majazunnabi@gcuf.edu.pk

https://doi.org/10.15251/JOR.2024.206.803

Zn-Cd ferrites are significant materials due to interesting properties such as their bulk composition exhibits anti-ferromagnetism but their nano composition exhibits ferrimagnetism. Unique physiochemical properties of spinel ferrites are greatly regulated by various factors such as their microstructure, synthesis rout, distribution of cations and dopant etc. Lot of research work has been done to improve electrical and dielectric properties by doping rare earth metals in parent compounds [10].

Many studies have been reported regarding influence of doping rare earth's metals on structural, electrical and dielectric parameters of spinel ferrites. Ali et al., reported that Conductivity and dielectric constant were increased when Ni-Zn ferrites substituted by Sn [11]. Lakshmi et al., reported that AC conductivity and dielectric constant were increased when Zn ferrites were doped with Cr [12]. Variation in electrical and structural traits of Ni-Cd spinel ferrites was studied and reported by Shelar et al. [13]. Arshad et al. described that lattice constant was increased for La doped Ni-Cd ferrites [14]. Vinod et al. synthesized Dy substituted Cu-Cd ferrites and reported that with the doping of Dy content, a significant increase in the dc electrical resistivity of the as- synthesized materials was observed [15]. Arshad et al. also examined the influence of Mg doping on Cd-Cu ferrites and found a reduced dielectric constant and ac conductivity with increasing contents of Mg [16]. Sikder et al. prepared the Eu doped Co-Ni-Zn spinel ferrites for applications in high frequency devices and reported that dielectric magnetic quality factors improved with the doping of Eu in the spinel lattice replacing Fe^{3+} cations [17]. Arshad et al. studied the effects of lanthanum (La^{3+}) on the properties of Mg-Cd-Cu ferrites. They found the energy gap to range from 2.95 to 3.38 eV. Electrical resistivity measurements indicated that the ferrites exhibited semiconducting behavior. The sample with a La^{3+} concentration of $x = 0.05$ displayed the highest magnetic parameters, while the sample with $x = 0.025$ showed the maximum resistivity [18]. Mustafa et al. investigated the impact of lanthanum (La) doping on nickel ferrites. They noted random variations in the lattice constant, attributed to strain and the larger ionic radius of lanthanum. The dielectric parameters showed consistent behavior in the microwave frequency range, indicating that these materials are suitable for microwave device applications [19]. Ikram et al. examined the effects of lanthanum (La^{3+}) ion substitution on the properties of Ni-Zn-Cd ferrites. The incorporation of La^{3+} ions significantly modified the structural, dielectric, and magnetic characteristics of $Ni_{0.5}Zn_{0.3}Cd_{0.2}Fe_{2-\gamma}La_{\gamma}O_4$ (with y ranging from 0.0 to 0.21). They found that both saturation magnetization and retentivity decreased with increasing La^{3+} ion content. [20].

The present study focuses on simplistic synthesis of La^{3+} and Er^{3+} rare earth metal cations co-doped Zn- Cd ferrites via SGAC technique, to study the structural, electrical and dielectric characteristics for various technological applications in the microwave and radio frequency range. Various fabrication methods such as co-precipitation, Ball-milling method, ceramic method and sol-gel auto-combustion route have been utilized to fabricate spinel ferrites. Due to suitable compositional control, less time in synthesis procedure, cost effectiveness, homogeneous mixing of the components, greater possibility of multi component oxides which consist of single phase having high surface area, SGAC technique was chosen to prepare ferrite nanoparticles in the present study [21-23].

2. Experimental details

Zn-Cd ferrites substituted with La^{3+} and Er^{3+} cations having compositional formula $Zn_{0.5}Cd_{0.5}Fe_{1.9}La_{0.1-x}Er_xO4$ ($x = 0 - 0.1$ with an interval of 0.02) were fabricated by SGAC technique. After weighing stoichiometrically, metal nitrates $Cd(NO_3)_3.4H_2O$, $Zn(NO_3)_2.6H_2O$, $La(NO_3)_3.H_2O$, $Fe(NO_3)_3.9H_2O$, $Er(NO_3)_3.6H_2O$ were dispersed in distilled water seperately. $C_6H_8O_7$ (Citric acid) was used as a burning agent to achieve auto-combustion reaction in the ratio 1:1.2. Prepared solution of nitrates and citric acid was kept on magnetic stirrer where NH_4OH was added gradually until the solution's pH was reached to 7. Solution was then stirred continuously for 2 hours at 80 °C to attain homogeneity. Temperature of the homogenous solution gradually increased to 250 ℃ after formation of gel till the combustion achieved. The fluffy powder was grinded and calcinated two times at 550 ℃ and 750 °C for 2 and 8 hours in a muffle furnace respectively to achieve improved microstructure and crystalline nature. Calcinated samples were grinded about 30 minutes per sample by using agate-mortar and pestle. The prepared samples were examined by using various characterization techniques like X-ray diffraction (XRD), Fourier Transform Infrared spectroscopy (FTIR), and LCR measurements.

3. Results and discussions

3.1. XRD measurements

XRD analysis was employed to measure structural parametes of all synthesized ferrites. XRD powder patterns for all ferrites were plotted (Fig. 1) and then indexed by observing prominent peaks at different angles such as 2Θ = 29.7°, 35.1°, 42.8°, 53.2° and 56.53°. The hkl values are assigned to prominent diffracted peaks by comparing with JPCD card no.123345.

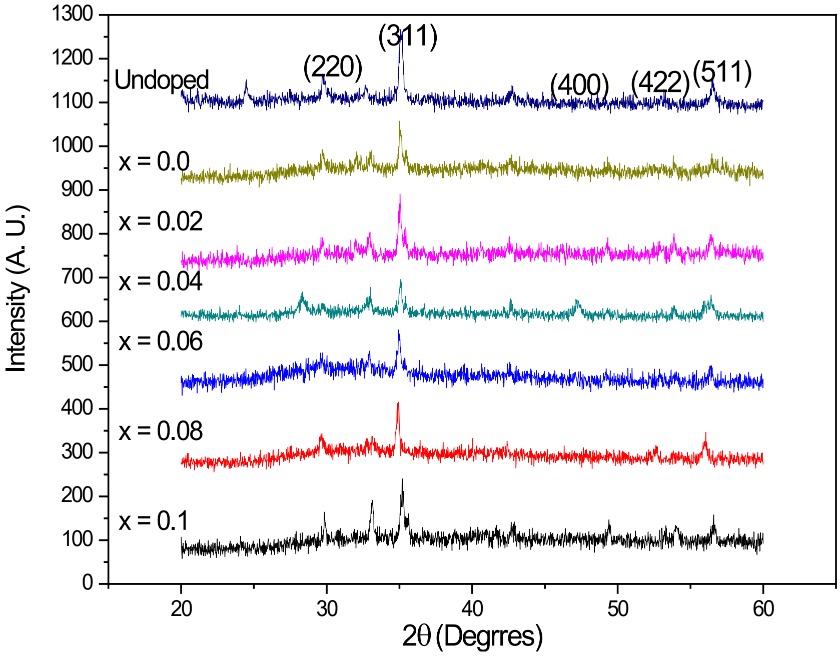

Fig. 1. XRD patterns of La^{3+} and Er^{3+} doped Zn-Cd spinel ferrites.

Table 1. Calculated XRD parameters and composition of samples.

Ferrite composition	Lattice constant (a)(Å)	Average crystallite size (D) (nm)	X-ray density (D_X) (g/cm^3)
$Zn_{0.5}Cd_{0.5}Fe_2O_4$	8.48	26.46	5.77
$Zn_{0.5}Cd_{0.5}Fe_{1.9}La_{0.1}O_4$	8.50	29.32	4.70
$Zn_{0.5}Cd_{0.5}Fe_{1.9}La_{0.08}Er_{0.02}{}^{o}{}_{4}$	8.49	29.13	5.93
$Zn_{0.5}Cd_{0.5}Fe_{1.9}La_{0.06}Er_{0.04}{}^{o}{}_{4}$	8.49	35.34	5.95
$Zn_{0.5}Cd_{0.5}Fe_{1.9}La_{0.04}Er_{0.06}{}^{o}{}_{4}$	8.49	35.07	5.97
$Zn_{0.5}Cd_{0.5}Fe_{1.9}La_{0.02}Er_{0.08}{}^{o}{}_{4}$	8.51	45.89	5.93
$Zn_{0.5}Cd_{0.5}Fe_{1.9}Er_{0.1}O_4$	8.49	46.23	5.81

From these peaks, spinel structure for all synthesized nano ferrites was confirmed. Some peaks indicating the presence of secondary phases also appeared in pattern. Different physical parameters such as lattice constant (a), crystallite size (D) and x-ray density (Dx) were determined by analyzing XRD results and are presented in Table 1. 'a' was estimated by employing the following relation

$$a = dhkl \times (h_2 + k_2 + l_2)^{1/2} \tag{1}$$

where hkl indicate the miller indices and 'd_{hkl}' represents inter-planer spacing. Lattice constant for un-doped sample is 8.484 Å which is closed to previous reported values. This value increased slightly by inclusion of La^{3+} ions which may be because of larger ionic radius of La^{3+} (1.65 Å) as compared to host site Fe^{3+} (0.65 Å) and enlarges the spinel lattice of the sample. Further for x = 0.02-0.06, lattice constant decreased gradually which may be because of the substitution Er^{3+}. As we increased Er^{3+} content (having ionic radii 0.9 Å) and decreased La^{3+} content (having ionic radii 1.65 Å) so addition of smaller atoms in the place of larger atoms should cause a decrease in lattice constant and same behavior can be noticed for samples up to x = 0.06. For x = 0.08 - 0.1, lattice constant exhibited an un-expected behavior which may be because of the substitution of rare earth's ions on grain boundaries [24-25]. 'D' was calculated using Scherer formula

$$D = (0.9 \times \lambda)/ \beta \cos\theta \tag{2}$$

'D' was found in the range 26-46 nm as shown in Fig. 2. Un-doped sample exhibited the crystallite size of 26 nm which have a great resemblance with the value reported in the literature [7,21]. The value increased to 29 nm by inclusion of La^{3+} ions and can be attributed to proper diffusion of La^{3+} ions into spinel lattice which leads to proper grain growth. A slight decrease was observed for sample with x = 0.02 which can be because of the disturbance in the lattice due to addition of Er^{3+} ions and diffusion of La^{3+} ions on interstitial sites [26-28]. Following relation was used to determine x-ray density (Dx).

$$D_x = 8 \times M/V \times N_a \tag{3}$$

here 'M' represents the molar mass of samples, 'Na' the Avogadro's number and 'V' represents volume of crystals of samples which can be calculated from lattice constants 'a' using relation

$$V = a \times a \times a \tag{4}$$

From the above equations, X-ray density 'D_x' is related to molar mass and value of lattice constant and trend obtained from calculations is similar to the changes in mass and lattice constant. The values of D_x are presented in Table 1 and have range 4.70 g/cm^3 to 5.97 g/cm^3.

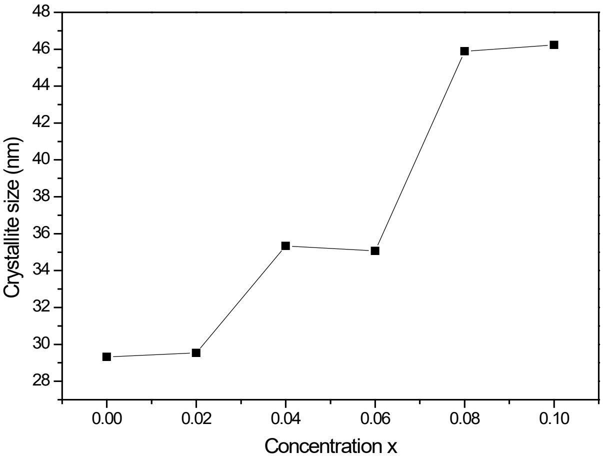

Fig. 2. Plot of crystallite size vs. concentration.

3.2. FTIR measurements

FTIR is an important characterization technique which provides information regarding structure of the material and is helpful in obtaining information regarding the molecular bonding and vibration modes existing in the materials. The FTIR spectra of all the prepared samples are depicted in Fig. 3. Two absorption bands of 408 – 425 cm^{-1} and 525 – 550 cm^{-1} were observed as low and high frequency bands respectively. Two distinct absorption bands were observed named high frequency band υ_1 (525-550 cm^{-1}) and low frequency band υ_2 (408-425 cm^{-1}). Waldron [29] suggested that vibrational frequencies in the range of 600-500 cm^{-1} are linked to the Fe^{3+}-O^{2-} complex at tetrahedral sites, while frequencies between 450-350 cm^{-1} are associated with Fe^{3+}-O^{2-} and M^{2+}-O^{2-} complexes at octahedral sites. From this, we can infer that the high-frequency absorption band (υ1) arises from the stretching vibrations of metal-oxide bonds at tetrahedral sites, while the low-frequency absorption bands are due to stretching vibrations of metal-oxide bonds at octahedral sites [26,30]. These observed bands confirm the formation of a spinel structure in our samples.

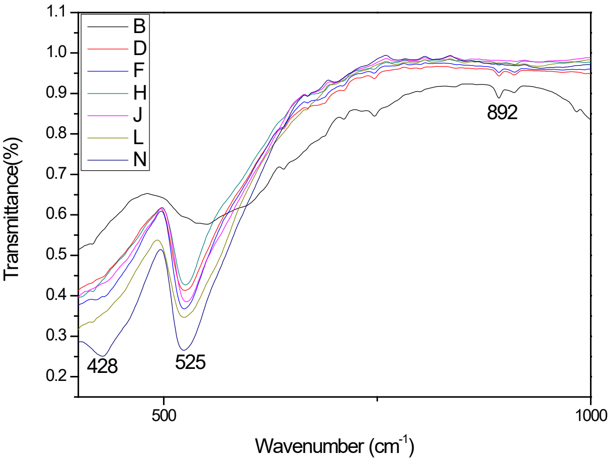

Fig. 3. FTIR spectra of rare earth substituted Zn-Cd ferrites.

3.3. LCR measurements

The dielectric performance of spinel nanoferrites are significantly affected by a number of factors, including synthesis methods, particle size, ion distribution in interstitial sites, sintering temperature, stoichiometric composition, the ratio of Fe^{3+} to Fe^{2+} ions, and oxygen deficiencies [31]. To explore how varying the content of rare earth (RE^{3+}) ions impacts dielectric parameters such as dielectric constant (ε'), dielectric loss (ε''), AC conductivity, and Q value—measurements were taken on the synthesized spinel ferrites across a frequency range of 8 Hz to 8 MHz, all at room temperature

Fig. 4 displays the variations of dielectric constant (ε') with frequency for the synthesized spinel ferrites. Across all samples, dielectric constant (ε') exhibited larger values at smaller frequencies and decreased with further increase in frequency gradually, eventually becoming saturated at higher frequencies. At high frequency, reduction in dielectric constant may be because of the incapability of the hopping mechanism to keep pace with the external electric field, causing any polarization effects at these higher frequencies to lag behind the electric field. This polarizing effect could result from changes in the valence states of cations [9]. The frequency-dependent response of the dielectric parameters can be further clarified by Maxwell-Wagner model and Koop's theory [9,32-34]. An irregular trend was observed for different concentrations of rare earth dopants, which may be credited to variations in cationic distributions, porosity, and grain size. Additionally, these irregularities in the dielectric constant with varying composition may also be due to differences in crystallite size, as per Koops' model, where the polarization of the crystal lattice becomes the dominant contributor to the dielectric constant at higher frequencies [35].

The frequency dependent behavior of dielectric loss ($\varepsilon^{//}$) is displayed in Figure. 5. Observed dielectric loss exhibited a decreasing trend with frequency. Various factors such as structural inhomogeneity and non-stoichiometric etc. can influence the dielectric loss. This frequency dependent behavior has a great accordance with the Koop’s theory. Electrical conduction and dielectric behavior of spinel ferrites are strongly correlated with each other so increasing applied field’ frequency causes an increase in resistivity through the grain boundaries which leads to a decrease in dielectric loss [36]. It also can be seen that the sample for x = 0 has high dielectric loss and sample for x = 0.02 has low dielectric loss.

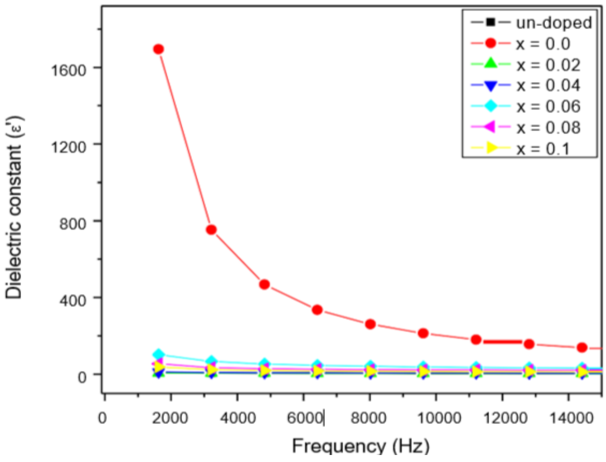

Fig. 4. Frequency vs dielectric constant (ε’).

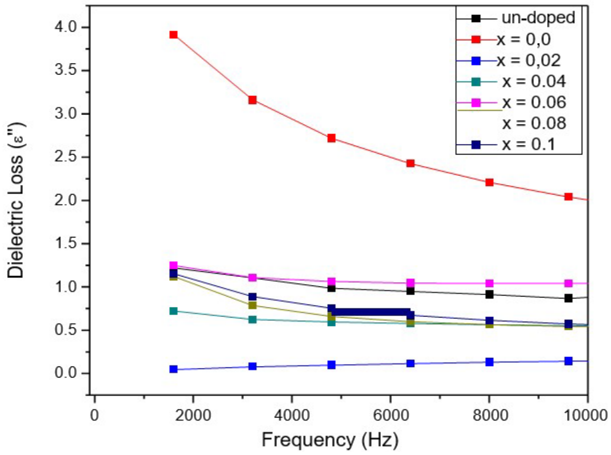

Fig. 5. Frequency versus dielectric loss (ε’’).

Figure 6 illustrates the variation of impedance with frequency, based on measurements taken at room temperature using an LCR meter across the frequency range of 4 Hz to 8 MHz. The graph reveals a decreasing trend in the real part of the impedance (Z') with increase in frquency. This reduction is due to the space charge polarization phenomenon in the synthesized oxide materials. At lower frequencies, Z' exhibits a higher magnitude, likely due to the predominant hopping mechanism between iron ions. The observed decline in the real part of the impedance at higher frequencies is likely a result of increased conductivity [37].

Figure 7 illustrates how conductivity varies with frequency. It shows that conductivity increases as frequency rises, likely due to higher frequencies facilitating electron hopping between Fe^{3+} and Fe^{2+} ions. Consequently, this results in the observed increase in conductivity. Notably, the samples with 'x = 0' and 'x = 0.06' demonstrate higher conductivity values compared to the others, possibly because the hopping mechanism responds more effectively to the applied frequency in these cases. In contrast, the lower conductivity values for the other samples could be attributed to the doping of Er^{3+} ions, which reduces the number of Fe^{3+} ions and isolates them to a degree that decreases the probability of charge hopping [38-40].

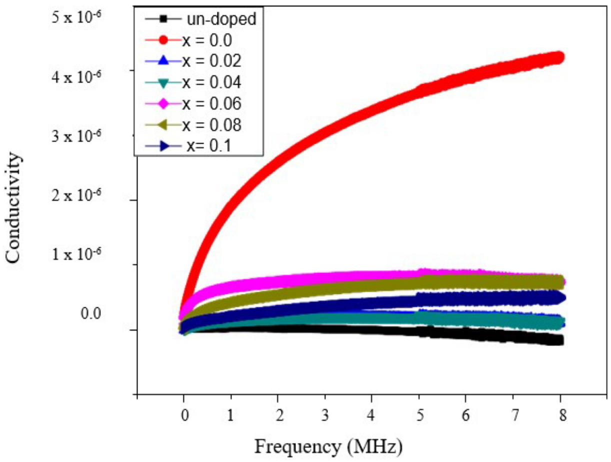

Fig. 6. Plot of AC conductivity vs. frequency.

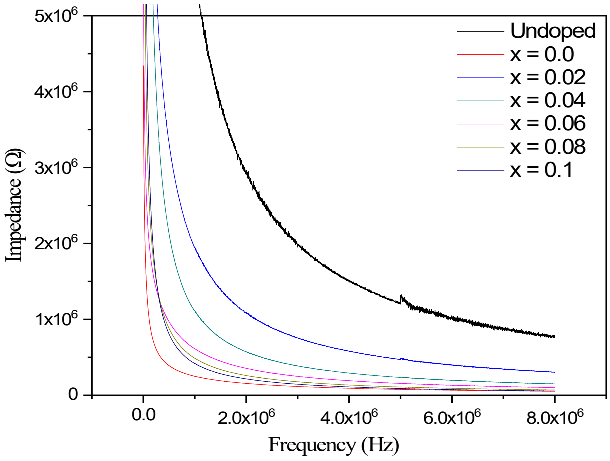

Fig. 7. Frequency versus real part of impedance.

4. Conclusions

A series of seven spinel ferrites with general formula $Zn_{0.5}Cd_{0.5}Fe_{1.9}La_{0.1-x}Er_xO_4$, (where x = 0 - 0.1 with a step interval of 0.02) was fabricated by sol-gel auto-combustion technique. Grown samples were double calcinated at 550 and 750 ℃ for 2 and 8 hours, respectively. Spinel structure was confirmed from XRD powder pattern but with additional phase. The lattice constant derived from the XRD results showed a decreasing trend with increasing concentration, ranging from 8.85 to 8.51 Å. Meanwhile, the average crystallite size varied from 26 to 46 nm and displayed an increasing trend with concentration. Two major absorption bands, low frequencies and high frequencies were observed from FTIR analysis lie in range 400-430 cm^{-1} and 500-550 cm^{-1}. Lower frequency band shifted to higher frequency when concentration increased. Dielectric constant for sample x = 0 increased to 1694 and irregularity was found for other concentrations. Dielectric constant and dielectric loss increased for lower frequency but decreased for higher frequencies.

Acknowledgments

The authors would like to acknowledge Researcher's Supporting Project Number (RSP2024R511), King Saud University, Riyadh, Saudi Arabia.

Conflicts of interest

The authors declare no conflict of interest.

Data availability

Data will be made available on request.

References

[1] S. Atiq, M. Majeed, A. Ahmad, S.K. Abbas, M. Saleem, S. Riaz, S. Naseem, Ceramics International 43, 2486 (2017); https://doi.org/10.1016/j.ceramint.2016.11.046

[2] K.V. Kumar, A.C.S. Reddy, D. Ravinder, Journal of Magnetism and Magnetic Materials 263, 121 (2003); https://doi.org/10.1016/S0304-8853(02)01544-5

[3] S. Mukherjee, S. Pradip, A.K. Mishra, D. Das, Applied Physics A 116, 389 (2014); https://doi.org/10.1007/s00339-013-8140-2

[4] Q. Liu, L. Lv, J.-P. Zhou, X.-M. Chen, X.-B. Bian, P. Liu. Journal of Ceramic Processing Research 13, 110 (2012).

[5] A. Ghasemi, M. Mousavinia. Ceramics International 40, 2825 (2014); https://doi.org/10.1016/j.ceramint.2013.10.031

[6] F. Yi. Ceramics International 40, 7837 (2014); https://doi.org/10.1016/j.ceramint.2013.12.128

[7] M. Abbas, B.P. Rao, M.N. Islam, K.W. Kim, S.M. Naga, M. Takahashi, C. Kim, Ceramics International 40, 3269 (2014); https://doi.org/10.1016/j.ceramint.2013.09.109

[8] C.B. Carter, M.G. Norton, Ceramic Materials-Science and Engineering, Springer, (2013); https://doi.org/10.1007/978-1-4614-3523-5

[9] M. Ashtar, A. Munir, M.A.-U. Rehman, A. Maqsood, Materials Research Bulletin 79, 14 (2016); https://doi.org/10.1016/j.materresbull.2016.02.044

[10] N.U. Khan, N. Amin, M.U. Khalid, M. Amami. M.A.U. Nabi, Materials Science and Engineering: B 308, 117580 (2024); https://doi.org/10.1016/j.mseb.2024.117580

[11] M.A. Ali, M.M. Uddin, M.N.I. Khan, F.-U.-Z. Chowdhry, S.M. Haque, Journal of Magnetism and Magnetic Materials 424, 148 (2017); https://doi.org/10.1016/j.jmmm.2016.10.027

[12] M. Lakshmi, K.V. Kumar, K. Thyagarajan, Advances in Materials Physics and Chemistry 6, 141 (2016); https://doi.org/10.4236/ampc.2016.66015

[13] M.B. Shelar, P.A. Jadhav, S.S. Chougule, M.M. Mallapur, B.K. Chougule, Journal of Alloys and Compounds 476, 760 (2009); https://doi.org/10.1016/j.jallcom.2008.09.107

[14] M.I. Arshad, S. Ikram, K. Mahmood, A. Ali, M.A.U. Nabi, N. Amin, Y. Arooj, N. Sawaira, M. Asghar, M. Saleem, F. Jabeen, J. Batool, G. Mustafa, Journal of Ovonic Research 14, 27 (2018).

[15] G. Vinod, K. Rajashekhar, J.L. Naik, Ceramics International 49, 2829 (2023); https://doi.org/10.1016/j.ceramint.2022.09.265

[16] M.I. Arshad, S. Arshad, K. Mahmood, A. Ali, N. Amin, U.U. Rehman, M. Isa, A. Akram, N. Sabir, M.A.U. Nabi, Physica B: Condensed Matter 599, 412496 (2020); https://doi.org/10.1016/j.physb.2020.412496

[17] M.S. Sikder, M.D. Hossain. I. Sardar. M.S. Hossain, M.N.I. Khan. M.R. Rahman, Results in Physics 46, 106320 (2023); https://doi.org/10.1016/j.rinp.2023.106320

[18] MI. Arshad, MS. Hasan, AU. Rehman, M. Akhtar, N. Amin, K. Mahmood, NTK. Thanh, Ceramics International, 48, 14246 (2022); https://doi.org/10.1016/j.ceramint.2022.01.313

[19] G. Mustafa, M. Khalid, AD Chandio, K. Shahzadi, Z. Uddin, JK. Khan, HNHK. Asghar, Journal of Sol-Gel Science and Technology, 101, 596 (2022); https://doi.org/10.1007/s10971-020-05359-z

[20] S. Ikram, J. Jacob, MI. Arshad, K. Mahmood, A. Ali, N. Sabir, S. Hussain, Ceramics International, 45, 3563 (2019); https://doi.org/10.1016/j.ceramint.2018.11.015

[21] A. Manzoor, M.A. Khan, M. Shahid, M.F. Warsi, Journal of Alloys and Compounds 710, 547 (2017); https://doi.org/10.1016/j.jallcom.2017.03.154

[22] M.U. Khalid, R. Kousar, M.I. Arshad, N. Amin, S.M. Siddeeg, M. Amami, M. Ahmad, M. Ibrar, M.A.U. Nabi, Materials Chemistry and Physics 323, 129639 (2024); https://doi.org/10.1016/j.matchemphys.2024.129639

[23] S. Nag, A.R. Chowdhry, D. Das, S. Das, S. Mukherjee, Journal of Magnetism and Magnetic Materials 466, 172 (2018); https://doi.org/10.1016/j.jmmm.2018.06.084

[24] Y.M.A. Angari, Journal of Magnetism and Magnetic Materials 323, 1835 (2011); https://doi.org/10.1016/j.jmmm.2011.02.003

[25] V. Chaudhari, S.E. Shirsath, M.L. Mane, R.H. Kadam, S.B. Shelke, D.R. Mane, Journal of Alloys and Compounds 549, 213 (2013); https://doi.org/10.1016/j.jallcom.2012.09.060

[26] A.B. Gadkari, T.J. Shinde. P.N. Vasambekar, Journal of Alloys and Compounds 509, 966 (2011); https://doi.org/10.1016/j.jallcom.2010.08.155

[27] S. Prathapani, M. Vinitha, T.V. Jayaraman, D. Das, Journal of Applied Physics 115, 17A502 (2014); https://doi.org/10.1063/1.4854915

[28] K. Rajashekhar, G. Vinod, K.M. Kumar, J.L. Naik, Journal of Magnetism and Magnetic Materials 555, 169323 (2022); https://doi.org/10.1016/j.jmmm.2022.169323

[29] R. Waldron, Physical Reviews 99, 1727 (1955); https://doi.org/10.1103/PhysRev.99.1727

[30] M. Deepty, C. Srinivas, E.R. Kumar, N.K. Mohan, C.L. Prajapat, T.V.C. Rao, S.S. Meena, A.K. Verma, D.L. Sastry, Ceramics International 45, 8037 (2019); https://doi.org/10.1016/j.ceramint.2019.01.029

[31] M.Y. Lodhi, K. Mahmood, A. Mahmood, H. Malik, M.F. Warsi, I. Shakir, M. Asghar, M.A. Khan, Current Applied Physics 14, 716 (2014); https://doi.org/10.1016/j.cap.2014.02.021

[32] K.M. Batoo, G. Kumar, Y. Yang, Y. Al-Douri, M. Singh, R.B. Jotania, A. Imran, Journal of Alloys and Compounds 726, 179 (2017); https://doi.org/10.1016/j.jallcom.2017.07.237

[33] S.G. Kakade, R.C. Kambale, Y.D. Kolekar, C.V. Ramana, Journal of Physics and Chemistry of Solids 98, 20 (2016); https://doi.org/10.1016/j.jpcs.2016.03.015

[34] K.M. Batoo, S. Kumar, C.G. Lee, Alimuudin, Current Applied Physics 9, 826 (2009); https://doi.org/10.1016/j.cap.2008.08.001

[35] R. Ali, M.A. Khan, A. Mahmood, A.H. Chugtai, A. Sultan, M. Shahid, M. Ishaq, M.F. Warsi, Ceramics International 40, 3841 (2014); https://doi.org/10.1016/j.ceramint.2013.08.024

[36] M.B. Mohamed, Applied Physics A 125, 756 (2019); https://doi.org/10.1007/s00339-019-2492-1

[37] M.A. Al-Mamun, M.S.I. Sarker, M.R. Hasan, M.M. Haque, F.A. Khan, M.M. Rahman. M.K.R. Khan, Results in Physics 29, 104698 (2021).

[38] S. Sharma, J.M. Siqueiros, O.R. Herrera, Journal of Alloys and Compounds 853, 156979 (2021); https://doi.org/10.1016/j.jallcom.2020.156979

[39] P. Pandit, S. Satapathy, P. Sharma, P.K. Gupta, S.M. Yousaf, V.G. Sathe; Bulletin of Materials Science 34, 899 (2011); https://doi.org/10.1007/s12034-011-0212-3

[40] S. Ikram, J. Jacob, K. Mehboob, K. Mahmood, N. Amin, M.I. Arshad, M.A.U. Nabi, Journal of Superconductivity and Novel Magnetism 34, 1833 (2021); https://doi.org/10.1007/s10948-020-05688-8